environmental microbiology

Environmental Microbiology (2017) **00**(00), 00–00 doi:10.1111/1462-2920.13662

Evolution of copper resistance in the kiwifruit pathogen *Pseudomonas syringae* pv. *actinidiae* through acquisition of integrative conjugative elements and plasmids

Elena Colombi,[1]* Christina Straub,[1] Sven Künzel,[2] Matthew D. Templeton,[3,4] Honour C. McCann[1,5†] and Paul B. Rainey[1,2,6†]

[1]*New Zealand Institute for Advanced Study, Massey University, Auckland, New Zealand.*

[2]*Max Planck Institute for Evolutionary Biology, Plön, Germany.*

[3]*Plant and Food Research, Auckland, New Zealand.*

[4]*School of Biological Sciences, University of Auckland, Auckland, New Zealand.*

[5]*South China Botanical Institute, Chinese Academy of Sciences, Guangzhou, China.*

[6]*Ecole Supérieure de Physique et de Chimie Industrielles de la Ville de Paris (ESPCI Paris-Tech), PSL Research University, Paris, France.*

Summary

Horizontal gene transfer can precipitate rapid evolutionary change. In 2010 the global pandemic of kiwifruit canker disease caused by *Pseudomonas syringae* pv. *actinidiae* (*Psa*) reached New Zealand. At the time of introduction, the single clone responsible for the outbreak was sensitive to copper, however, analysis of a sample of isolates taken in 2015 and 2016 showed that a quarter were copper resistant. Genome sequences of seven strains showed that copper resistance – comprising *czc*/*cusABC* and *copABCD* systems – along with resistance to arsenic and cadmium, was acquired via uptake of integrative conjugative elements (ICEs), but also plasmids. Comparative analysis showed ICEs to have a mosaic structure, with one being a tripartite arrangement of two different ICEs and a plasmid that were isolated in 1921 (USA), 1968 (NZ) and 1988 (Japan), from *P. syringae* pathogens of millet, wheat and kiwifruit respectively. Two of the *Psa* ICEs were nearly identical to two ICEs isolated from kiwifruit leaf colonists prior to the introduction of *Psa* into NZ. Additionally, we show ICE transfer *in vitro* and *in planta*, analyze fitness consequences of ICE carriage, capture the *de novo* formation of novel recombinant ICEs, and explore ICE host-range.

Received 18 August, 2016; accepted 2 January, 2017. *For correspondence. E-mail e.colombi@massey.ac.nz, Tel. (+64) 9 4140800 ext 43810. †Joint senior authors.

Introduction

Horizontal gene transfer (HGT) is a potent evolutionary process that significantly shapes patterns of diversity in bacterial populations. Horizontally transmissible elements, including plasmids, phages and integrative conjugative elements (ICEs) move genes over broad phylogenetic distances and mediate abrupt changes in niche preferences that may even fuel speciation (Griffith, 1928, Médigue *et al.*, 1991; Lan and Reeves, 1996; Sullivan and Ronson, 1998; Ochman *et al.*, 2000; Ochman *et al.*, 2005; Retchless and Lawrence, 2007; Guglielmini *et al.*, 2011; Popa and Dagan, 2011; Polz *et al.*, 2013).

ICEs are plasmid-like entities with attributes of temperate phages that disseminate vertically as part of the bacterial chromosome and horizontally by virtue of endogenously encoded machinery for conjugative transfer (Wozniak and Waldor, 2010; Guglielmini *et al.*, 2011). Essential genetic modules include those mediating integration, excision, conjugation and regulation of conjugative activity (Mohd-Zain *et al.*, 2004; Juhas *et al.*, 2007; Roberts and Mullany, 2009). During the process of conjugation ICEs circularize and transfer to new hosts, leaving a copy in the original host genome (Wozniak and Waldor, 2010; Johnson and Grossman, 2015). Conjugation during pathogenesis is often regulated by environmental signals (Lovell *et al.*, 2009; Quiroz *et al.*, 2011; Vanga *et al.*, 2015).

In addition to a set of essential genes, ICEs often harbour 'cargo' genes of adaptive significance to their hosts. These include genes affecting biofilm formation, pathogenicity, antibiotic and heavy metal resistance, symbiosis and bacteriocin synthesis (Peters *et al.*, 1991; Rauch and De Vos, 1992; Ravatn *et al.*, 1998; Beaber *et al.*, 2002;

Drenkard and Ausubel, 2002 ; Burrus *et al*., 2006; Ramsay *et al*., 2006; Dimopoulou *et al*., 2007; Kung *et al*., 2010). The genetic information stored in cargo genes varies considerably resulting in ICEs that range in size from 20 kb to 500 kb (Johnson and Grossman, 2015).

In 2008, a distinct and particularly virulent form of the kiwifruit pathogen *Pseudomonas syringae* pv. *actinidiae* (*Psa*) was identified in Italy. It was subsequently disseminated throughout kiwifruit growing regions of the world causing a global pandemic that reached New Zealand (NZ) in 2010 (Balestra *et al*., 2010; Abelleira *et al*., 2011; Everett *et al*., 2011; Vanneste *et al*., 2011). Genomic analysis showed that although the pandemic was derived from a single clone it acquired a set of distinctive ICEs during the course of its global journey (Mazzaglia *et al*., 2012; Butler *et al*., 2013; McCann *et al*., 2013). The NZ lineage carries *Psa*$_{NZ13}$ICE_eno which harbours a 20 kb 'enolase' region' that is also found in otherwise divergent *Psa* ICEs (McCann *et al*., 2013; McCann *et al*., 2017).

Copper sprays have long been used in NZ to protect plants from a range of diseases. Since the arrival of *Psa* in NZ kiwifruit orchardists have employed copper-based products to protect vines. From 2011, an ongoing industry-based programme has been in place to monitor copper resistance. In 2014, evidence was first obtained of *Psa* isolates resistant to copper sulphate. Given that the clone of *Psa* originally introduced into NZ was sensitive to copper and lacked genes encoding copper resistance (McCann *et al*., 2013), detection of copper resistance raised the possibility that this is an evolutionary response to the use of copper-based sprays.

Here, we report the phenotypic and genetic basis of copper resistance into NZ isolates of *Psa* and show that its emergence has been fuelled by HGT involving ICEs and plasmids. We additionally describe the mosaic structure of ICEs, show the dynamics of ICE transfer both *in vitro* and *in planta*, analyze fitness consequences of ICE carriage, capture the *de novo* formation of novel recombinant ICEs and explore ICE host-range.

Results

Occurrence of copper resistance in Psa

Psa NZ13, isolated in 2010 and representative of the clone introduced into NZ, lacks genes encoding copper resistance (McCann *et al*., 2013) and is unable to grow at copper concentrations in excess of 0.8 mM $CuSO_4$ on MGY. Prior to 2014 no copper resistant or tolerant *Psa* strains had been reported in NZ. However, in 2014, two strains isolated from two different kiwifruit orchards, *Psa* NZ45 and *Psa* NZ47, displayed copper resistance, with a MIC of 1.2 mM $CuSO_4$. This finding prompted a small-scale sampling of both copper treated and untreated orchards in 2015/2016 encompassing the area where resistance was first identified. From a sample of 213 strains isolated from seven orchards 59 were found to be copper resistant. Copper resistant isolates were recovered from both copper treated and untreated orchards. Additional copper resistant strains were procured from other kiwifruit-growing regions of NZ (Supporting Information Fig. S1).

ICE and plasmid-mediated acquisition of copper resistance in Psa

The genome of the focal copper resistant isolate, *Psa* NZ45, is a direct clonal descendant of the isolate originally introduced into NZ (*Psa* NZ13) with 2 SNPs in the 4,853,155 bp non-recombinant core genome alignment (McCann *et al*., 2017), but differs in two significant regards. First, the 'native' ICE (*Psa*$_{NZ13}$ICE_eno) at *att-1* (immediately upstream of *clpB*) is located at the second *att* site (*att-2*) immediately downstream of *queC* (Fig. 1). Second, the genome harbours a new 107 kb ICE (*Psa*$_{NZ45}$ICE_Cu) integrated at the *att-1* site: *Psa*$_{NZ45}$ICE_Cu carries genes encoding copper resistance (Figs 1 and 2A).

The genomes of six additional copper resistant *Psa* isolates were also sequenced (Table 1) and as with *Psa* NZ45, reads were aligned against the *Psa* NZ13 reference genome (McCann *et al*., 2013; Templeton *et al*., 2015). All six harbour mobile elements carrying genes encoding copper resistance. The diversity of these elements and genomic location is shown in Fig. 1 and their structure is represented in Fig. 2A. All isolates are direct clonal descendants of *Psa* NZ13 and thus share an almost identical genome with the exception of the determinants of copper resistance. In *Psa* NZ47, the genes encoding copper resistance are located on a 90 kb ICE (*Psa*$_{NZ47}$ICE_Cu) integrated at the *att-1* site: the native *Psa*$_{NZ13}$ICE_eno is located at the *att-2* site. *Psa* NZ62 carries an ICE identical to that found in *Psa*$_{NZ47}$ICE_Cu (*Psa*$_{NZ62}$ICE_Cu), but is integrated at the *att-2* site; the native ICE (*Psa*$_{NZ13}$ICE_eno) is absent leaving the *att-1* site unoccupied. Isolate *Psa* NZ63 carries *Psa*$_{NZ45}$ICE_Cu integrated at the *att-1* site, but, the native *Psa*$_{NZ13}$ICE_eno has been lost. Copper resistance genes in isolate *Psa* NZ64 are also ICE-encoded, but the NZ64 ICE (*Psa*$_{NZ64}$ICE_Cu) is genetically distinct from both *Psa*$_{NZ47}$ICE_Cu and *Psa*$_{NZ45}$ICE_Cu – at 130 kb, it is also the largest. In NZ64, *Psa*$_{NZ64}$ICE_Cu is located at the *att-1* site and the *att-2* site contains the native (*Psa*$_{NZ13}$ICE_eno) ICE. Isolates *Psa* NZ65 and NZ66 both harbour copper resistance genes on a near identical, 120 kb previously undescribed plasmid (pPsaNZ65 and pPsaNZ66 respectively). The only significant difference among the plasmids is the location of a strepomycin resistance-encoding transposon (see below): both isolates have the original *Psa*$_{NZ13}$ICE_eno integrated at the *att-2* site (Fig. 1). *Psa* harbouring copper

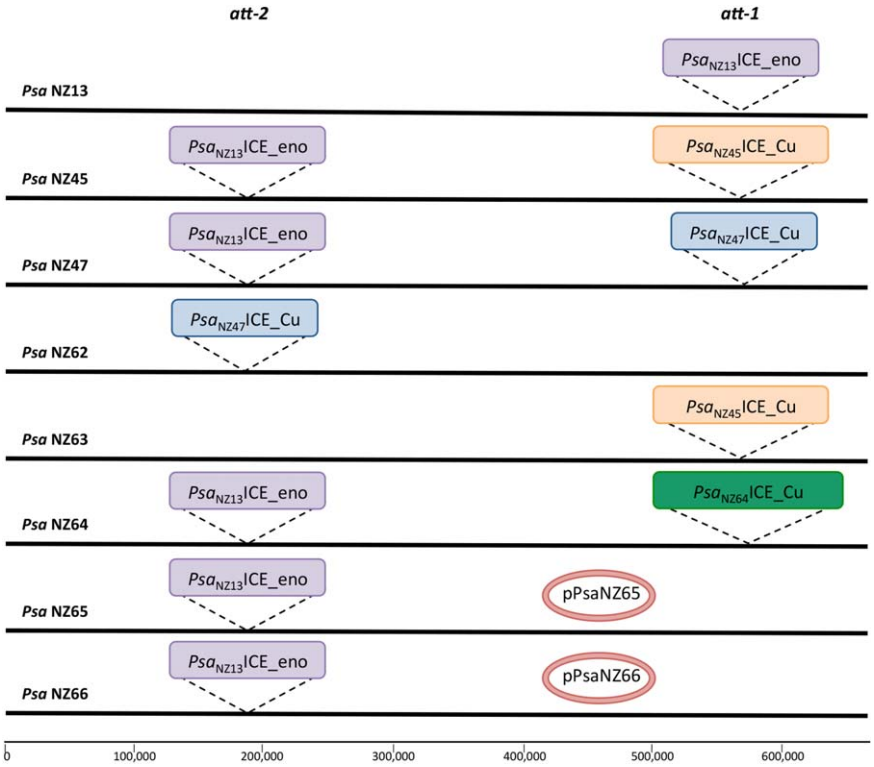

Fig. 1. Genomic location of *Psa*ICEs. In purple the Psa_{NZ13}ICE_eno (100 kb), in orange Psa_{NZ45}ICE_Cu (107 kb), in blue the Psa_{NZ47}ICE_Cu (90 kb), in green the Psa_{NZ64}ICE_Cu (130 kb), pPsaNZ65 and pPsaNZ66 plasmids are 111 kb. Each island is bounded by 52 bp *att* sequences overlapping tRNALys. In *Psa* NZ13 the *att-1* site is located at 5,534,632 bp, *att-2* at 1,733,972 bp. The figure is not to scale (the entire genome of 6.7 Mbp is indicated as a single black line). Both Psa_{NZ13}ICE_eno and Psa_{NZ47}ICE_Cu ICEs were detected in *Psa* NZ47 by sequencing, but analysis of independent colonies from the freezer stock show that Psa_{NZ13}ICE_eno is prone to loss.

resistance-encoding ICEs have a MIC $CuSO_4$ of 1.2 mM while the MIC of plasmid-carrying *Psa* is 1.5 mM (Table 1).

That such a small sample of isolates is each unique with regard to the copper resistance-encoding element points to highly dynamic processes shaping their evolution. Such dynamism has been previously noted among enolase-encoding ICEs obtained from a global collection of epidemic *Psa* isolates (McCann *et al.*, 2013) and has been observed elsewhere (Burrus *et al.*, 2006; Wozniak and Waldor, 2010). In this study, our samples came from a relatively small geographical location. Two ICEs, Psa_{NZ64}ICE_Cu and Psa_{NZ47}ICE_Cu, were found in different isolates sampled from the same orchard (one year apart), although the two isolates containing near identical plasmids were isolated from orchards located 100 km apart. Two isolates sampled one year apart from the same location (neighboring orchards in Te Puke) carry the same ICE (Psa_{NZ45}ICE_Cu = Psa_{NZ63}ICE_Cu; Psa_{NZ47}ICE_Cu = Psa_{NZ62}ICE_Cu) (Table 1).

The dynamics of ICE evolution becomes especially evident when placed in the broader context possible by comparisons to ICEs recorded in DNA databases. The core genes of the copper resistance-encoding ICEs from NZ *Psa* isolates are syntenous with the core genes of the family of ICEs that includes PPHGI-1 (isolated in 1984 from bean in Ethiopia (Teverson, 1991; Pitman *et al.*, 2005)) and the three ICEs previously described from *Psa* found in New Zealand (2010), Italy (2008) and China (2010) (McCann *et al.*, 2013; Butler *et al.*, 2013; E. Colombi, unpublished). Psa_{NZ45}ICE_Cu is a mosaic of DNA from two known ICEs and a plasmid. It shares regions of near perfect identity (over 66 kb) with ICEs present in the otherwise divergent host genomes of *P. syringae* pv. *panici* (*Ppa*, LGM2367) isolated from proso millet in Madison (USA) in the 1920s (over the first 38 kb it differs by just 12 SNPs, and one 144 bp indel), *P. syringae* pv. *atrofasciens* (*Paf*, ICMP4394) isolated in NZ in 1968 from wheat and a 70.5 kb plasmid present in a non-pandemic *Psa* strain (J2), isolated in Japan in 1988 (Fig. 2B).

Two of the ICEs described here have also been found in non-*Psa Pseudomonas* isolated from kiwifruit leaves. Psa_{NZ47}ICE_Cu shows 99.7% pairwise nucleotide identity with an ICE found in *P. marginalis* ICMP 11289 isolated in 1991 from *A. deliciosa* in Katikati (NZ). Psa_{NZ64}ICE_Cu is almost identical (99.5% nucleotide pairwise identity) to an ICE from *P. syringae* pv. *actinidifoliorum* (*Pfm*) ICMP19497, isolated from kiwifruit in 2010 in Te Puke (NZ) (Visnovsky *et al.*, 2016) (Table 1). Additionally, a 48 kb segment of Psa_{NZ64}ICE_Cu encoding copper resistance genes shares 99.3% nucleotide pairwise identity with a locus found in *P. azotoformans* strain S4 (Fang *et al.*, 2016), which was isolated from soil in 2014 in Lijiang (China). However, the locus from *P. azotoformans* is not associated with an ICE.

Genetic determinants of copper resistance

Copper resistance is typically conferred by operons encoding either copper efflux (*cusABC*) and/or sequestration

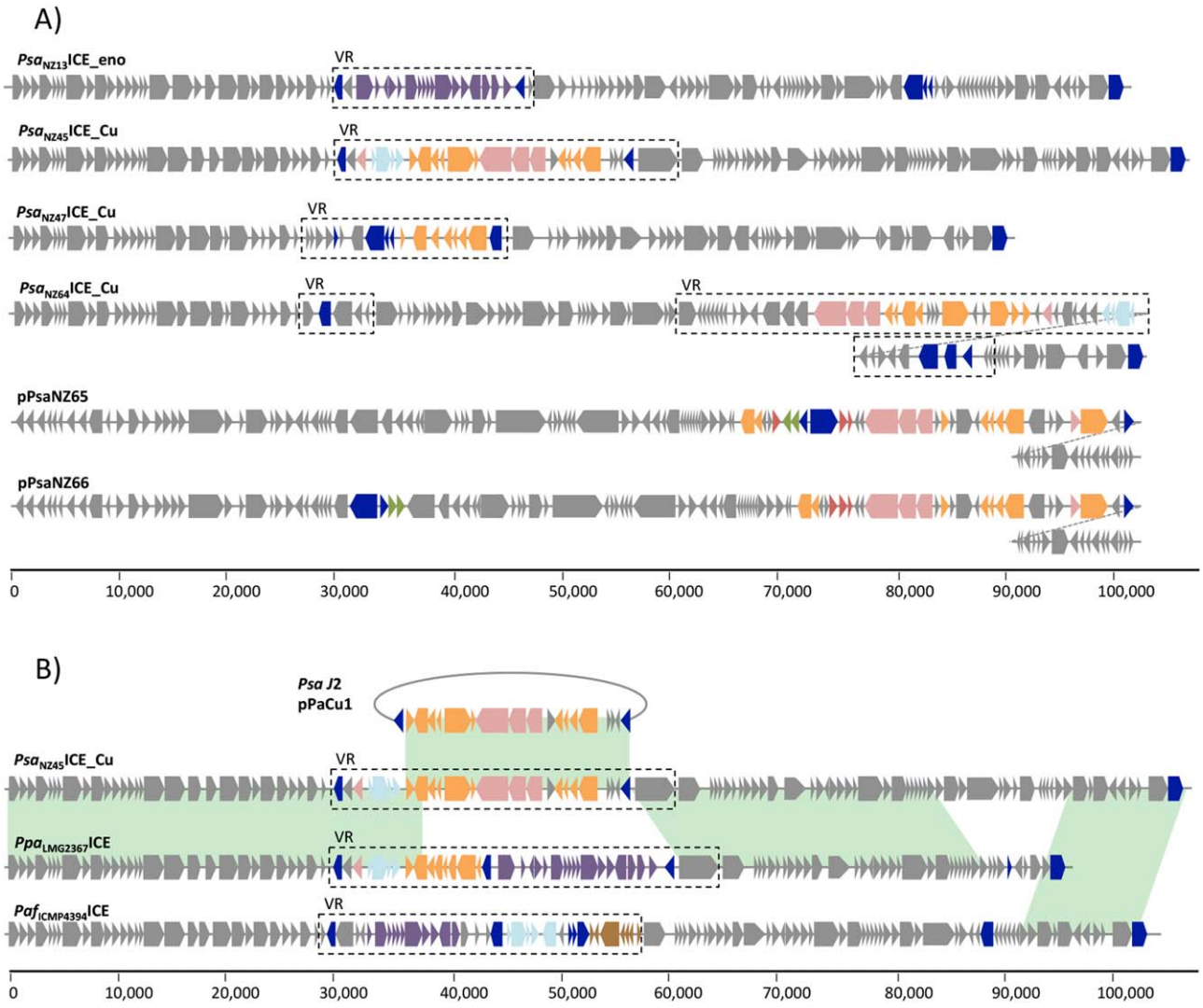

Fig. 2. Genetic organization of ICEs and plasmids acquired by *Psa* and mosaicism of Psa_{NZ45}ICE_Cu.
A. Blue boxes are mobile genes (transposases or recombinases), purple boxes define the 'enolase region', orange boxes depict copper resistance genes, azure boxes are arsenic resistance genes, pink boxes are genes belonging to the *czc*/*cus* system, green boxes are streptomycin resistance genes, red boxes are cation transporter ATPases, brown boxes denote genes encoding mercury resistance. Core 'backbone' and other cargo genes are depicted as grey boxes. Dotted diagonal lines indicate continuation of the element.
B. Areas in green show more than 99% pairwise nucelotide identity. Psa_{NZ45}ICE_Cu and $Ppa_{LGM2367}$ICE share identity both in the first 38 kb and 20 kb downstream of VR. The remaining 20 kb of the Psa_{NZ45}ICE_Cu VR is almost identical to pPaCu1 (it differs by just 2 SNPs). The last 12.5 kb of Psa_{NZ45}ICE_Cu is identical to $Paf_{ICMP4394}$ICE.

(*copABCD*) systems, both of which can be under the regulation of the *copRS*/*cusRS* two-component regulatory system (Bondarczuk and Piotrowska-Seget, 2013). ICEs identified in *Psa* isolates harbour operons encoding examples of both resistance mechanisms (and regulators), plus genetic determinants of resistance to other metal ions. In each instance, the resistance genes are located within 'variable regions' (VR) of ICEs into which cargo genes preferentially integrate (Fig. 2A). Delineation of these variable regions comes from detailed analysis of 28 unique ICEs from the *Pph* 1302A and *Psa* families that will be published elsewhere (E. Colombi, unpublished). Overall there are notable similarities and differences in the organization of the variable regions.

As shown in Fig. 2B, the first 38 kb of Psa_{NZ45}ICE_Cu is almost identical (99.7% identical at the nucleotide level) to $Ppa_{LGM2367}$ICE. This region spans the core genes, but extends ~8.2 kb into the variable cargo genes with just two SNPs distinguishing the two ICEs (across the 8.2 kb variable region). Encoded within this region is an integrase, arsenic resistance genes (*arsRBCH*), a gene implicated in cadmium and cobalt resistance (*czcD*) and the *copRS*

Table 1. List of genomes used in this study.

Isolate ID	Place of Isolation	Year of Isolation	Host of Isolation	Orchard's copper Programme	MIC to $CuSO_4$	GenBank Accession	ICMP number
***Psa* NZ13**	Te Puke, NZ	2010	Kiwifruit	NA	0.8 mM	CP011972-3	18884
***Psa* NZ45**	Te Puke, NZ	2014	Kiwifruit	Full spray	1.2 mM	CP017007-8	20586
***Psa* NZ47**	Te Puke, NZ	2014	Kiwifruit	Spray free	1.2 mM	CP017009-11	22180
***Psa* NZ62**	Te Puke, NZ	2015	Kiwifruit	Organic	1.2 mM	MOMK00000000	22181
***Psa* NZ63**	Te Puke, NZ	2015	Kiwifruit	To minimum	1.2 mM	MOML00000000	22182
***Psa* NZ64**	Te Puke, NZ	2016	Kiwifruit	Spray free	1.2 mM	MOMM00000000	22183
***Psa* NZ65**	Te Puke, NZ	2016	Kiwifruit	Full spray	1.5 mM	MOMN00000000	22184
***Psa* NZ66**	Coromandel, NZ	2016	Kiwifruit	Full spray	1.5 mM	MOMJ00000000	22185
***Ppa* LGM2367**	Madison, USA	1921–1922	Proso millet	NA	NA	ALAC00000000	
***Paf* ICMP4394**	Auckland, NZ	1968	Wheat	NA	NA	LJPO00000000	4394
***P. marginalis* ICMP4394**	Katikati, NZ	1991	Kiwifruit	NA	NA	LKGX00000000	4394
***Psa* J2**	Japan	1988	Kiwifruit	NA	NA	AGNQ00000000	
***Pfm* ICMP19497**	Te Puke, NZ	2010	Kiwifruit	NA	NA	LKBQ00000000	19497

regulatory system. Partway through *copS* the two ICEs diverge at a recombination breakpoint with the downstream variable region from Psa_{NZ45}ICE_Cu being homologous to a set of copper resistance genes found on plasmid pPaCu1 from the divergent (non-pandemic) Japanese isolate of *Psa* (J2) (Nakajima *et al.*, 2002). This region comprises a putative copper transporting ATPase encoded by *copG* (Gutiérrez-Barranquero *et al.*, 2013), *cusABC* genes involved in the detoxification of monovalent cations, including copper and silver (Mergeay *et al.*, 2003; Rensing and Grass, 2003) and *copABCD* (Fig. 2B). The last 4 kb of the variable region of Psa_{NZ45}ICE_Cu shares almost complete identity with $Ppa_{LGM2367}$ICE (Fig. 2B).

Detail of the diversity of copper resistance (and related metal resistance) genes is shown in Fig. 3. All elements (ICEs and plasmids) harbour the *copRS* regulatory system and, with the exception of Psa_{NZ47}ICE_Cu, all carry both *cusABC* and *copABCD*, although their organization varies. For example, while *copABCD* is typical, in Psa_{NZ64}ICE_Cu *copAB* and *copCD* are organized as two separate operons (Fig. 3). The putative copper ABC transport system encoded by *copG* is a common feature, and determinants

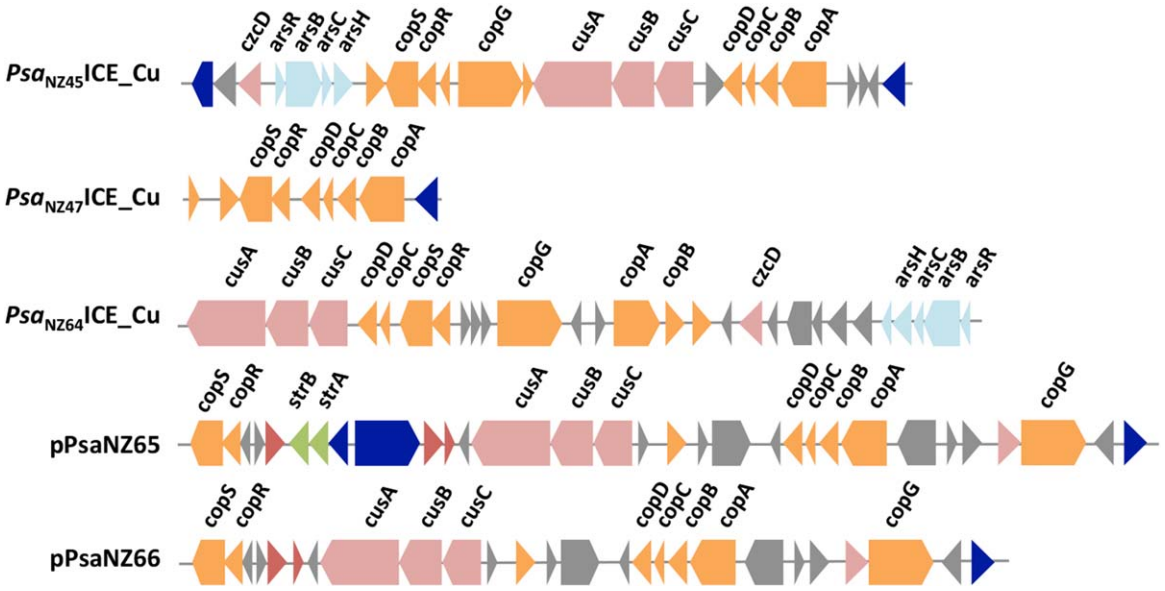

Fig. 3. Genetic organization of metal resistance loci. Blue boxes are mobile genes (transposases or recombinases), orange boxes depict copper resistance genes, azure boxes are arsenic resistance genes, pink boxes are genes belonging to the *czc/cus* system, green boxes are streptomycin resistance genes and other genes are depicted as grey boxes.

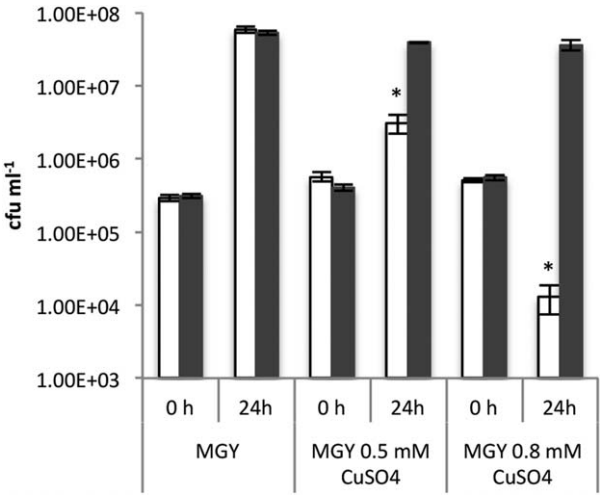

Fig. 4. Effect of copper ions on growth of *Psa* NZ13 and *Psa* NZ45. *Psa* NZ13 (white bars) and *Psa* NZ45 (grey bars) were grown for 24 h in shaken MGY culture and MGY supplemented with 0.5 mM and 0.8 mM $CuSO_4$. Data are means and standard deviation of three independent cultures. The asterisk indicates significant difference $P < .05$ (one tailed *t*-test)).

of arsenic resistance are present in both Psa_{NZ45}ICE_Cu and Psa_{NZ64}ICE_Cu. The putative cadmium and related metal resistance gene, *czcD*, is also present on these two ICEs. As noted above, a transposon carrying determinants of streptomycin resistance (*strAB*) is present on plasmids pPsaNZ65 and pPsaNZ66. The transposon is of the Tn*3* family and the cassette bears identity to streptomycin resistance carrying transposons found in *P. syringae* pv. *syringae* B728a (Feil *et al*., 2005), but also on plasmid pMRVIM0713 from *Pseudomonas aeruginosa* strain MRSN17623 (GenBank: KP975076.1), plasmid pPMK1-C from *Klebsiella pneumoniae* strain PMK1 (Stoesser *et al*., 2014) and plasmid pTi carried by *Agrobacterium tumefaciens* LBA4213 (Ach5) (GenBank: CP007228.1).

At the level of the operons determining copper resistance there is marked genetic diversity, however, with the exception of CopR, there is little evidence of within operon recombination. The CusABC system is carried on pPsaNZ65 and pPsaNZ66 (but these are identical) and the ICEs Psa_{NZ45}ICE_Cu and Psa_{NZ64}ICE_Cu: CusA, CusB and CusC show 75.8%, 50.0% and 44.8% pairwise amino acid identity respectively; phylogenetic trees based on protein sequences show congruence (Supporting Information Fig. S2). The CopABCD system is present on Psa_{NZ45}ICE_Cu, Psa_{NZ47}ICE_Cu, Psa_{NZ64}ICE_Cu (but CopAB and CopCD are in different locations (Fig. 3)) and plasmid pPsaNZ65 (and pPsaNZ66): CopA, CopB, CopC and CopD show 76.4%, 63.1%, 79.1% and 60.8% pairwise amino acid identity respectively. With the exception of CopC (where bootstrap support is low) phylogenetic trees for each protein show the same overall arrangement (Supporting Information Fig. S3). The two component regulatory system *copRS* is also present on each of the elements with the amino acid sequences of CopR showing 84.3% and those of CopS 63.0% pairwise amino acid identity. Phylogenetic trees show CopS from Psa_{NZ64}ICE_Cu to be the most divergent, and those from Psa_{NZ45}ICE_Cu and Psa_{NZ47}ICE_Cu being most similar: CopR shows the same phylogenetic arrangement, however, CopR sequences from Psa_{NZ45}ICE_Cu and Psa_{NZ47}ICE_Cu are identical at the protein level suggesting a recent recombination event (Supporting Information Fig. S4).

Psa_{NZ45}*ICE_Cu imposes no detectable fitness cost and confers a selective advantage* in vitro *in the presence of copper*

To determine whether ICE carriage confers a fitness cost, we took advantage of the fact that *Psa* NZ13 and *Psa* NZ45 are essentially isogenic, with the exception of the additional ICE in *Psa* NZ45 (Psa_{NZ45}ICE_Cu). Each strain was grown alone and density of cells monitored over a 72 h period with samples taken every 24 h. In the absence of copper sulphate, no difference in cell density was detected; however, in the presence of 0.5 and 0.8 mM $CuSO_4$ the density of *Psa* NZ13 was reduced (Fig. 4). There is thus no apparent fitness cost associated with carriage of Psa_{NZ45}ICE_Cu in the absence of copper sulphate, but there is a fitness advantage in copper-containing environments.

Although carriage of Psa_{NZ45}ICE_Cu appeared not to affect the growth of *Psa* NZ45 in the absence of copper, a more precise measure of fitness was sought by performing competition experiments in which *Psa* NZ13 and *Psa* NZ45 were co-cultured. For this experiment *Psa* NZ13 was marked with a kanamycin resistance cassette so that it could be distinguished from kanamycin sensitive, copper resistant *Psa* NZ45. Over a 24 h period where the two strains (founded at equal density) competed for the same resources (in shaken MGY medium without copper sulphate), the fitness of *Psa* NZ45 was not significantly different to *Psa* NZ13 (0.29 ± 0.2; mean and SEM from three independent experiments, each comprised of three replicates), indicating no significant detectable cost of carriage of Psa_{NZ45}ICE_Cu.

Given that the mechanism of copper resistance in *Psa* NZ45 – based upon *copABCD* – likely involves sequestration of copper ions we considered the possibility that this isolate might confer cross protection to non-copper resistant isolates, such as *Psa* NZ13. To this end, we performed co-culture experiments at sub-inhibitory and inhibitory copper sulphate concentrations. Growth of *Psa* NZ13 at sub-inhibitory concentrations of copper sulphate was significantly impaired by the presence of *Psa* NZ45

and this was especially evident at 48 and 72 h (Supporting Information Fig. S5). At the inhibitory copper sulphate concentration, *Psa* NZ13 appeared to benefit from the presence of *Psa* NZ45. Again, this was most evident at 48 and 72 h (Supporting Information Fig. S5).

Psa$_{NZ45}$*ICE_Cu imposes no detectable fitness cost but confers a minor selective advantage* in planta

Cost and benefit of carrying *Psa*$_{NZ45}$ICE_Cu was also evaluated during endophytic colonization of kiwifruit leaves. No significant difference was observed in growth of singly-inoculated *Psa* NZ13 and *Psa* NZ45 in both the absence and presence of a commonly used commercial copper-based product (Nordox75 (0.375 g l^{-1})) (Supporting Information Fig. S6). Competition assays in the presence or absence of Nordox75 confirmed carriage of *Psa*$_{NZ45}$ICE_Cu imposes no significant fitness cost or advantage during endophytic growth (Fig. 5 and Supporting Information Fig. S7). However, in the presence of Nordox75 there was a significant advantage to epiphytic cells carrying *Psa*$_{NZ45}$ICE_Cu observable at day 3, but not at day 7 (Fig. 5 and Supporting Information Fig. S7).

Psa$_{NZ45}$*ICE_Cu transfer dynamics* in vitro *and* in planta

To determine whether *Psa*$_{NZ45}$ICE_Cu is active and capable of self-transmission samples from the *Psa* NZ45 and *Psa* NZ13 mixtures from the co-cultivation experiments were also plated on MGY medium containing both kanamycin and copper sulphate. Copper resistant, kanamycin resistant transconjugants were detected both *in vitro* and *in planta*. This means that a fraction of *Psa* NZ13 strains acquired *Psa*$_{NZ45}$ICE_Cu. These transconjugants marginally inflate the counts of *Psa* NZ45, however, the number of transconjugants (see below) was several orders of magnitude less that *Psa* NZ13, thus having no appreciable effect on the measures of relative fitness.

At 24 h in shaken MGY broth transconjugants were present at a frequency of $5.04 \pm 2.25 \times 10^{-3}$ per recipient cell (mean and SEM from three independent experiments, each comprised of three replicates). Analysis of samples from *in planta* experiments showed that at 3 days, transconjugants were present at a frequency of $2.05 \pm 0.63 \times 10^{-2}$ per recipient cell (mean and SEM from three independent experiments, each comprised of five replicates). On plants in the presence of Nordox (0. 375 g l^{-1}) the frequency of transconjugants was $9.37 \pm 1.56 \times 10^{-2}$ per recipient three days after inoculation (mean and SEM from three independent experiments, each comprised of five replicates). Transfer was also observed in M9 agar, on M9 agar supplemented with 0.5 mM $CuSO_4$, on M9 agar supplemented with a macerate of Hort16A fruit with transconjugants present (at 48 h) at a frequency of $2.16 \pm 0.9 \times 10^{-5}$, $1.11 \pm 0.4 \times 10^{-5}$ and $1.98 \pm 0.8 \times 10^{-5}$ per recipient cell respectively.

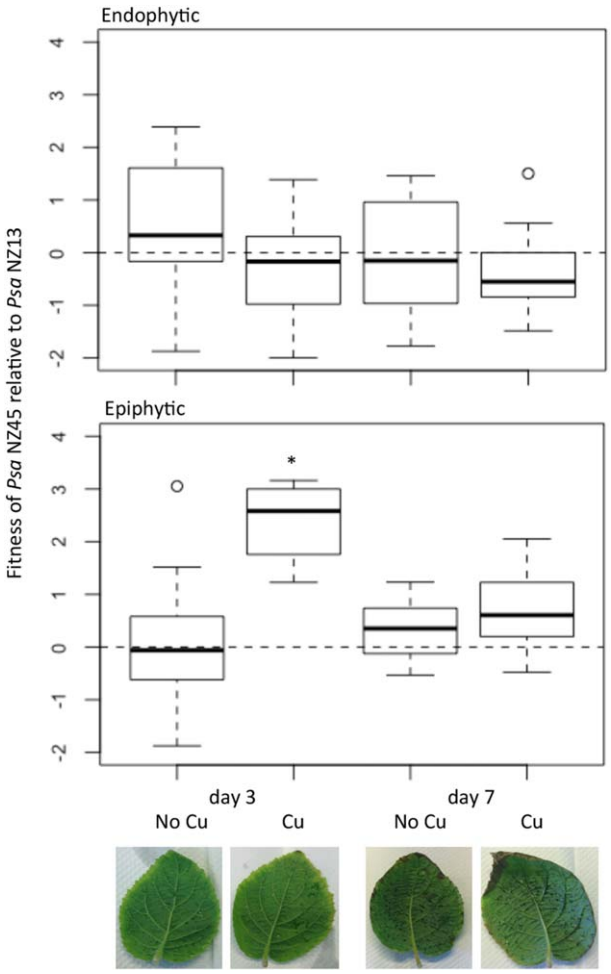

Fig. 5. Competition assay of *Psa* NZ45 and *Psa* NZ13 *in* and *super planta*. The difference in fitness between *Psa* NZ45 and *Psa* NZ13 was assessed endophytically and epiphytically on leaves of the kiwifruit cultivar Hort16A. Data represent the difference in the Malthusian parameters of three experiments of five replicates. The copper product Nordox75 (0.375 g L^{-1}) was sprayed adaxially and abaxially until run off (Cu). The asterisk indicates significant difference $P < .05$ from 0 (one tailed *t*-test)).

To explore the dynamics of transfer *in vitro*, samples from shaken MGY cultures were taken hourly, for 6 h, and then at 24 h. The data, presented in Fig. 6, show acquisition of *Psa*$_{NZ45}$ICE_Cu by *Psa* NZ13 within 1 h of the mating mix being established (approximately 1 recipient per 10^5 recipient cells). The frequency was relatively invariant over the subsequent 6 h period, but rose to approximately 1 recipient in 10^3 cells at 24 h.

Detection of ICE transfer just 1 h after mixing donor and recipient cells promoted a further experiment in which transconjugants were assayed at 10 min intervals. From three independent experiments, each with five replicates,

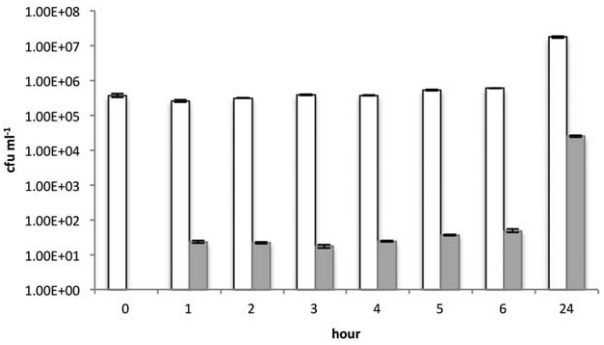

Fig. 6. *In vitro* transfer of Psa_{NZ45}ICE_Cu from *Psa* NZ45 to *Psa* NZ13. Colony forming units of the recipient *Psa* NZ13 (white bars) and *Psa* NZ13 carrying Psa_{NZ45}ICE_Cu (transconjugants, grey bars) was monitored during co-cultivation. Data are means and standard deviation of three independent cultures

transconjugants were detected at 30 min (approximately 4 $\times$ 10^{-7} transconjugants per recipient cell).

Analysis of co-cultivation experiments from kiwifruit leaves showed evidence that Psa_{NZ45}ICE_Cu also transferred *in planta*. The frequency of transconjugants at day 3 and day 7 was approximately 1 per 50 recipient cells and the frequency of transconjugants was not affected by changes in the initial founding ratios of donor and recipient cells (Supporting Information Table S1). Overall, the frequency of transconjugants was approximately three orders of magnitude greater *in planta* than *in vitro*.

ICE displacement and recombination

To check the genetic composition of transconjugants and to investigate whether Psa_{NZ45}ICE_Cu integration in recipient cells occurred at the *att-1* or *att-2* site, a set of primers were designed to identify the location of ICE integration in the *Psa* NZ13 genome (Supporting Information Table S2). Eleven independently generated transconjugants from shaken MGY culture were screened. As expected, successful amplification of primers annealing to *copABCD* in Psa_{NZ45}ICE_Cu was observed in all transconjugants, while amplification of the *enolase* gene primers (indicative of the presence of the native Psa_{NZ13}ICE_eno) occurred only in *Psa* NZ13 and *Psa* NZ45 (Supporting Information Fig. S8). However, in two transconjugants only the *IntPsaNZ13-att-1* primer pair resulted in amplification, suggesting that recombination between Psa_{NZ45}ICE_Cu and Psa_{NZ13}ICE_eno had occurred (Supporting Information Fig. S9). Genome sequencing of one of these transconjugants revealed a recombination event inside the variable region of the ICE that produced a chimeric ICE identical to Psa_{NZ45}ICE_Cu up to and including the CuR operon, with the remainder identical to the downstream segment of Psa_{NZ13}ICE_eno (Fig. 7).

Psa$_{NZ45}$*ICE_Cu can be transferred to a range of* P. syringae *strains*

The host range of the Psa_{NZ45}ICE_Cu was characterized using a panel of nine different *Pseudomonas* strains as recipients, representing the diversity of *P. syringae* and the genus more broadly. Transfer of Psa_{NZ45}ICE_Cu to *Psa* J31, *Pfm* NZ9 and *P. syringae* pv. *phaseolicola* (*Pph*) 1448a (on M9 agar plates) was observed with the frequency of transconjugants per recipient cell being 7.64 $\pm$ 1.7 $\times$ 10^{-6}, 7.74. $\pm$ 2.5 $\times$ 10^{-7} and 1.23 $\pm$ 0.2 $\times$ 10^{-4} respectively. No transconjugants were detected for *P. aeruginosa* PAO1, *P. fluorescens* SBW25, *P. syringae* pv. *tomato* DC3000 or *Psa* K28, despite the fact that these three strains have both *att* sites.

Discussion

The importance and impact of HGT on the evolution of microbial populations has long been recognized (Sullivan *et al*., 1995; Lilley and Bailey, 1997; Ochman *et al*., 2005; 2000; Wozniak and Waldor, 2010; Polz *et al*., 2013). Here we have captured the real time evolution of copper resistance in a plant pathogen, in an agricultural setting, and

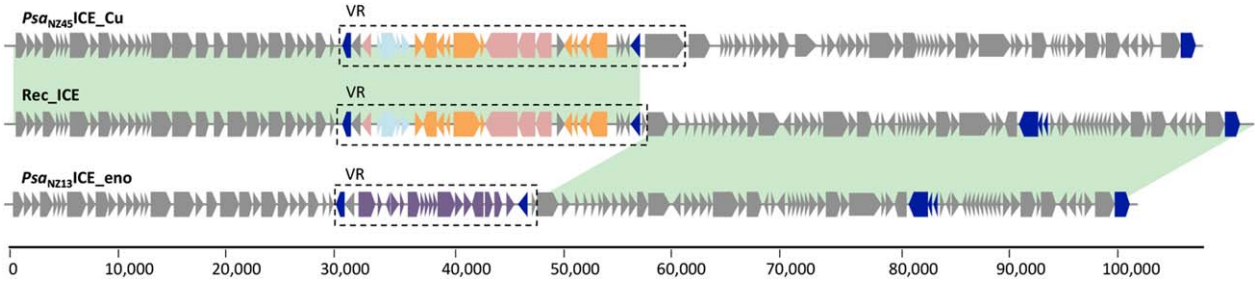

Fig. 7. Structure and mosaicism of the recombinant ICE (Rec_ICE) in transconjugant *Psa* NZ13. Areas highlighted in green show 100% pairwise identity. The recombination break point is inside the variable region (VR). Blue boxes are mobile genes (transposases or recombinases), purple boxes define the 'enolase region' (McCann *et al*. 2013), orange boxes depict copper resistance genes, azure boxes are arsenic resistance genes and pink boxes are genes belonging to the *czc*/*cus* system. Core 'backbone' and other cargo genes are depicted as grey boxes.

shown that movement of copper resistance genes occurs primarily via ICEs. Of the seven copper resistant *Psa* isolates analyzed, five contain copper resistance-encoding ICEs – three unique ICEs in total – with variable placement within the *Psa* genome, including movement and instability of the native ICE (Psa_{NZ13}ICE_eno). Further evidence of dynamism comes from *in vitro* and *in planta* studies, which show not only transfer to isogenic *Psa* and unrelated *P. syringae* strains, but also the ready formation of chimeras between Psa_{NZ45}ICE_Cu and Psa_{NZ13}ICE_eno. Mosaicism of ICEs has been reported elsewhere and is often promoted by the presence of tandem copies (Garriss *et al.*, 2009; Wozniak and Waldor, 2010). The ease with which ICEs move between strains and capacity for intra-ICE recombination emphasizes the futility of drawing conclusions on strain phylogeny based on ICE phylogeny (McCann *et al.*, 2013), but also the impossibility of understanding ICE evolution based on the phylogeny of ICEs themselves.

Evidence of the formation of chimeric ICEs extends beyond the ICEs studied here. Psa_{NZ45}ICE_Cu is a recombinant of two previously reported ICEs and a plasmid: most surprising is the fact that the recombinant components are derived from elements isolated from three geographic regions (USA, Japan and New Zealand) from three different plants (millet, kiwifruit and wheat) and spanning almost 100 years. Additionally, two of the copper resistance-encoding ICEs found in *Psa* (Psa_{NZ47}ICE_Cu and Psa_{NZ64}ICE_Cu) have been reported in other kiwifruit leaf colonizing organisms emphasizing the ease by which self-transmissible elements can move between members of a single community. Clearly, the potency of evolution fuelled by ICEs with the *P. syringae* complex is remarkable, with impacts likely extending well beyond that inferred from the analysis of genome sequences (Fondi *et al.*, 2016).

Evidence of the spectrum and dynamic of transfer inferred from the genomic analysis of natural isolates is bolstered by demonstration of the *in vitro* and *in planta* transfer of Psa_{NZ45}ICE_Cu. The fact that Psa_{NZ45}ICE_Cu can be detected in a recipient strain just 30 min after mixing with a donor strain (in shaken broth culture) points to an as yet undetermined proficiency for transfer. At the same time, the frequency of transconjugants *in planta* are several orders of magnitude greater than *in vitro* suggesting even greater potential for transfer in the natural environment.

The selective causes underpinning the evolution of copper resistance in *Psa* is uncertain and to date copper resistance in *Psa* is not known to have evolved outside of NZ. While it is tempting to blame use of copper sprays by orchardists, it is possible that the evolution of copper resistant *Psa* is a more general response to copper levels in New Zealand soils, copper emission to the atmosphere from anthropomorphic activities (Hong *et al.*, 1996; Staehlin *et al.*, 2016), combined with the use of copper-based sprays in NZ agriculture (Morgan and Taylor, 2004; Dean, 2016). Support for this stems from the fact that Psa_{NZ47}ICE_Cu shows almost perfect identify with an ICE found in *P. marginalis* (ICMP 11289) from kiwifruit isolated in 1991 (in NZ). In addition, copper resistance-encoding ICEs were found in both copper treated and untreated orchards.

In previous studies of copper resistance in *P. syringae*, beneficial effects due to carriage of resistance genes have been detected during assays of epiphytic growth (Sundin *et al.*, 1989; Menkissoglu and Lindow, 1991). In our work, the impact of the copper resistance-encoding ICEs on fitness *in planta* – in the presence of copper sprays – appears to be minimal. The selective advantage conferred by Psa_{NZ45}ICE_Cu was statistically significant only for epiphytic growth at day 3 in the presence of Nordox75. The lack of observable benefit at day 7 likely reflects tissue breakdown and escape of endophytic bacteria through stomata, causing inflation of the number of epiphytic bacteria (Fig. 5).

From the perspective of pathogen control using copper-based sprays there are at least three reasons to treat our detection of a minimal advantage to carriage of genetic determinants of copper resistance with caution. First, for reasons mentioned above and encountered elsewhere (Beattie and Lindow, 1999; Hirano and Upper, 2000) it is difficult to accurately assess fitness of microbes on plants and it is possible that our measures underestimate the contribution of copper resistance to growth in the presence of copper: even a 1% increase in fitness over 24 h, which is beyond experimental capacity to detect, can have significant long-term consequences. Second, the presence of copper resistance genes means opportunity for levels of resistance to increase through, for example, promoter mutations that increase levels of transcription of resistance determinants, or through acquisition of additional copper resistance-encoding genes. Third, and perhaps most significantly, is the fact that the copper resistance-encoding ICEs confer no measurable fitness cost even in the absence of copper. This suggests that these elements will not be readily lost from *Psa* populations even if copper-based sprays were eliminated (Andersson and Hughes, 2010; Neale *et al.*, 2016). That some strains of the global pandemic now contain two ICEs gives reason to suspect elevated evolutionary potential among these isolates.

While the focus of our investigation has been copper resistance, the ICEs reported here carry a cargo of additional genes, some of which are implicated in resistance to other metals. In some instances, the cargo genes have no similarity to genes of known function (some of the grey boxes in Fig. 2A). ICEs and similar laterally transferred elements provide opportunity for genes unrelated to copper resistance, for example gene connected to virulence, to hitchhike and rapidly spread. In this regard, the two plasmids characterized here are of interest: both carry

determinants of streptomycin resistance – an antibiotic that is also sprayed on NZ kiwifruit orchards in order to control *Psa*. The potential for hitchhiking has been previously noted in the context of antibiotic resistance-encoding plasmids (Gullberg *et al.*, 2014).

Recognition of ICEs along with their potential to change the course of microbial evolution extends less than twenty years (Wozniak and Waldor, 2010). While it might be argued that this potential is no different from that long realized via conjugative plasmids, or phage (Ochman *et al.*, 2000), ICEs, being a composite of both, seem to have an edge. Unlike conjugative plasmids that rarely integrate into the host genome, ICEs integrate as a matter of course and are largely immune to segregational loss; additionally, fitness consequences as a result of carriage are likely to be minimal. Unlike temperate phages, ICEs do not kill the host upon transfer, but they can nonetheless mediate transfer upon encountering transfer proficient conditions. Having control over both vertical and horizontal modes of transmission, while minimizing costs for host cells, marks these elements as especially potent vehicles of microbial evolution.

Experimental procedures

Strains and culture condition

All *Pseudomonas* strains were cultured in King's B medium at 28°C, *E. coli* was cultured in Luria Bertani medium at 37°C. All liquid overnight cultures were shaken at 250 rpm. Both kanamycin and nitrofurantoin were used at 50 μg ml^{-1}.

DNA extraction and genome sequencing

For genome sequencing, DNA samples were extracted using the Promega Wizard® Genomic DNA Purification Kit following the recommended protocol. *Psa* NZ45 was sequenced using the PacBio platform, the remainder were sequenced using the Illumina HiSeq platform.

Genomic reconstruction of ICEs

ICEs identified in genome sequences were used as query sequences for BLAST searches of the NCBI WGS database (http://blast.ncbi.nlm.nih.gov/Blast.cgi). Contigs were subsequently downloaded and where ICEs were represented by two contigs they were concatenated in Geneious (http://www.geneious.com, Kearse *et al.*, 2012). Concatenation was only required in two instances. ICEs were annotated using the RAST server (http://rast.nmpdr.org, Aziz *et al.*, 2008) and manually curated. Alignments were performed using Geneious.

Psa *isolation from kiwifruit orchards*

1 cm^2 kiwifruit leaf disks were macerated in 200 μl 10 mM $MgCl_2$. The macerate was plated on *Pseudomonas* selective media amended with cetrimide, fucidin and cephalosporin (Oxoid) and incubated at 28°C for 3 days. *Psa* was identified using either diagnostic PCR or LAMP assays (Rees-George *et al.*, 2010; Ruinelli *et al.*, 2017).

Copper resistance assays

Copper resistance was evaluated by determining the minimal concentration of copper that inhibited growth (minimal inhibitory concentration, MIC) on mannitol-glutamate yeast extract medium (MGY) plates supplemented with $CuSO_4{\cdot}5H_2O$ (Bender and Cooksey, 1986; Cha and Cooksey 1993). *Psa* strains were considered resistant when their MIC exceeded 0.8 mM $CuSO_4$.

Mutant development

A Tn*5* transposon was used to generate kanamycin resistant (*kanR*) strains. *E. coli* S17-1 Tn*5hah Sgid1* (Zhang *et al.*, 2015) was used as donor and *E. coli* pK2013 (Ditta *et al.*, 1980) as helper. Helper, donor and recipients were grown overnight. 200 μl of helper and donor and 2 ml of recipient were separately washed with 10 mM $MgCl_2$ and then mixed together and washed again. The mix was then re-suspended in 30 μl of 10 mM $MgCl_2$, plated on pre-warmed LB agar plates and incubated for 24–48 h at 28°C. Cells were then harvested, resuspended in 1 ml of sterile 10 mM $MgCl_2$ and plated on KB kanamycin nitrofurantoin plates. Selected mutants were screened for normal growth in KB, LB and M9.

In vitro *growth*

Overnight cultures of *Psa* NZ13^{kanR} and *Psa* NZ45 were used to determine the *in vitro* growth of each strain in MGY alone or supplemented with 0.5 and 0.8 mM $CuSO_4$. 10 ml liquid MGY cultures were established with a starting density of 10^5 cfu ml^{-1} and shaken for up to 3 days. Bacterial growth was monitored by plating on KB kanamycin (*Psa* NZ13^{kanR}), MGY 0.8 mM $CuSO_4$ (*Psa* NZ45). Three replicates per strain and media combination was used, and the experiment was repeated three times.

In planta *growth*

Clonally propagated *Actinidia chinensis* var. 'Hort16A' plantlets were maintained at 20°C with a light/dark period of 14/10 h, 70% constant humidity. *Psa* NZ13^{kanR} and *Psa* NZ45 were grown on KB agar plates for 48 h at 28°C. Inoculum with a final optical density (OD_{600}) of 0.2 of either strain was prepared in 50 ml 10 mM $MgCl_2$ with 0.002% of Silwet. Three to four week old plantlets were inoculated by dipping the aerial parts in the inoculum solution for 5 sec. Five separate plantlets were dip inoculated for each treatment. For experiments assessing *in planta* growth in copper-sprayed plantlets, Nordox75 was used at the recommended dosage of 0.375 g l^{-1} (www.kvh.org.nz/spray_products). Dip-inoculated plantlets were allowed to dry, then sprayed adaxially and abaxially with Nordox75 until runoff to ensure complete coverage. Bacterial growth was monitored 0, 3 and 7 days post inoculation. 1 cm^2 disk leaves were cut using a sterile cork borer, surface

sterilized in 70% ethanol and ground in 200 μl 10 mM $MgCl_2$. Serial dilutions of the homogenate were plated on KB kanamycin to count *Psa* NZ13^{kanR} and MGY 0.8 mM $CuSO_4$ to count *Psa* NZ45. Each experiment was repeated three times.

In vitro *and* in planta *competition assays*

In vitro and *in planta* competition assays were conducted as described earlier for single strains, except that *Psa* NZ45 and *Psa* NZ13^{kanR} were coinoculated in a 1:1 mix. Endophytic bacteria were harvested as above. To measure the epiphytic population, leaves were detached and the petiole sealed with wax. Each leaf was placed in a sterile bag containing 35 ml of 10 mM $MgCl_2$. Bags were gently shaken for 3 min, leaf washes were transferred into 50 ml centrifuge tubes and the solution centrifuged for 10 min at 4000 rpm. The supernatant was discarded and the pellet resuspended in 200 μl 10 mM $MgCl_2$. Bacterial growth was monitored by plating serial dilutions on KB kanamycin (*Psa* NZ13^{kanR}), MGY 0.8 mM $CuSO_4$ (*Psa* NZ45) and on MGY kanamycin 0.8 mM $CuSO_4$ (*Psa*NZ13^{kanR} that acquired copper resistance). *In vitro* assays had three replicates per strain, *in planta* assays were conducted using five replicates, each experiment was repeated three times. Fitness was calculated as the difference between their Malthusian Parameters: $\ln[N_{PsaNZ45}(t_1)/N_{PsaNZ45}(t_0)] - \ln[N_{PsaNZ13}(t_1)/N_{PsaNZ13}(t_0)]$ (Lenski *et al*., 1991).

ICE integration screening

Primers used in this study are listed in Supporting Information Table S2. Four primers were designed to detect the genomic location of ICE integration: two specific for the integrases at the end of each ICEs (*IntPsaNZ45*, *IntPsaNZ13*) and two for the ICE insertion site on the chromosome, annealing to the *clpB* (*att-1* site) and *queC* (*att-2* site) genes. The primer combination (*IntPsaNZ45-att-2*, *IntPsaNZ45-att-1, IntPsaNZ13-att-1* and *IntPsaNZ13-att-2*) indicates the location of the ICEs. Another two sets of primers were designed to amplify either CuR (*copA*) or enolase genes present in the VR of Psa_{NZ45}ICE_Cu and Psa_{NZ13}ICE_eno respectively. PCRs were performed using Thermo Scientific *Taq* DNA Polymerase following the manufacturer's instructions.

ICE mobilization assay

Psa NZ45 was used as the ICE donor. Strains tested in the mobilization assays are listed in order of divergence relative to the donor: *Psa* K28 (biovar 2) (McCann *et al*., 2013), *Psa* J31 (biovar 1) (McCann *et al*., 2013), *P. syringae* pv. *actinidifoliorum* NZ9 (McCann *et al*., 2013), *P. syringae* pv. *tomato* DC3000 (Buell *et al*., 2003), *P. syringae* pv. *phaseolicola* 1448a (Teverson, 1991), *P. syringae* H24 and H33 (isolated from kiwifruit; C. Straub, unpublished data), *P. fluorescens* SBW25 (Zhang *et al*., 2006) and *P. aeroginosa* PAO1 (Holloway, 1955). The copper sulphate MIC was determined for all tested recipient strains, which were all tagged with kanamycin Tn*5*. A biparental mating was performed using 2 ml and 200 μl of washed recipient and *Psa* NZ45 cells respectively. The cells were mixed, centrifuged briefly and resuspended in 30 μl of 10 mM $MgCl_2$ alone, 10 mM $MgCl_2$ with 0.5 mM $CuSO_4$ or 30 μl of 1 cm^2 kiwifruit plantlet macerate in 200 μl of 10 mM $MgCl_2$ as required. The cell mixture was plated onto solid media (M9 plates) and incubated at 28°C for 48 h. Cells were then harvested and resuspended in 1 ml of sterile 10 mM $MgCl_2$. Serial dilutions were plated on KB kanamycin to count the total number of recipients and on MGY amended with kanamycin and copper sulphate to count transconjugants.

Biosecurity and approval

All works were performed in approved facilities and in accord with APP201675, APP201730, APP202231.

Acknowledgements

Authors gratefully acknowledge Zespri International Limited and Te Puke Fruit Growers Association for financial support. The sponsors had no role in the design, collation, or interpretation of data. We thank kiwifruit growers in Te Puke for the access to orchards, Denis Robinson for providing Nordox75, and Daniel Rexin, Yunhao Liu and Kyosuke Yamamoto for assistance with isolating *Psa* from kiwifruit leaves.

References

Abelleira, A., López, M.M., Peñalver, J., Aguín, O., Mansilla, J.P., Picoaga, A., and García, M.J. (2011) First report of bacterial canker of kiwifruit caused by *Pseudomonas syringae* pv. *actinidiae* in Spain. *Plant Dis* **95:** 1583.

Andersson, D.I., and Hughes, D. (2010) Antibiotic resistance and its cost: is it possible to reverse resistance? *Nat Rev Microbiol* **8:** 260–271.

Aziz, R.K., Bartels, D., Best, A.A., DeJongh, M., Disz, T., Edwards, R.A., *et al*. (2008) The RAST Server: rapid annotations using subsystems technology. *BMC Genomics* **9:** 75.-10.1186/1471-2164-9-75.

Balestra, G.M., Renzi, M., and Mazzaglia, A. (2010) First report of bacterial canker of *Actinidia deliciosa* caused by *Pseudomonas syringae* pv. *actinidiae* in Portugal. *New Dis Rep* **22:** 10.

Beaber, J.W., Hochhut, B., and Waldor, M.K. (2002) Genomic and functional analyses of SXT, an integrating antibiotic resistance gene transfer element derived from *Vibrio cholerae*. *J Bacteriol* **184:** 4259–4269.

Beattie, G.A., and Lindow, S.E. (1999) Bacterial colonization of leaves: a spectrum of strategies. *Phytopathology* **89:** 353–359.

Bender, C.L., and Cooksey, D.A. (1986) Indigenous plasmids in *Pseudomonas syringae* pv. *tomato*: conjugative transfer and role in copper resistance. *J. Bacteriol* **165:** 534–541.

Bondarczuk, K., and Piotrowska-Seget, Z. (2013) Molecular basis of active copper resistance mechanisms in Gram-negative bacteria. *Cell Biol Toxicol* **29:** 397–405.

Buell, C.R., Joardar, V., Lindeberg, M., Selengut, J., Paulsen, I.T., Gwinn, M.L., *et al*. (2003) The complete genome sequence of the Arabidopsis and tomato pathogen *Pseudomonas syringae* pv. *tomato* DC3000. *Proc Natl Acad Sci USA* **100:** 10181–10186.

Burrus, V., Marrero, J., and Waldor, M.K. (2006) The current ICE age: biology and evolution of SXT-related integrating conjugative elements. *Plasmid* **55:** 173–183.

Butler, M.I., Stockwell, P.A., Black, M.A., Day, R.C., Lamont, I.L., and Poulter, R.T.M. (2013) *Pseudomonas syringae* pv. *actinidiae* from recent outbreaks of kiwifruit bacterial canker belong to different clones that originated in China. *PLoS One* **8:** e57464.

Cha, J.S., and Cooksey, D.A. (1993) Copper hypersensitivity and uptake in *Pseudomonas syringae* containing cloned components of the copper resistance operon. *Appl Environ Microbiol* **59:** 1671–1674.

Dean, F.P. (2016) Effects of Copper Sprays on Microbial Communities in Kiwifruit Orchard Soils. Doctoral dissertation. University of Waikato.

Dimopoulou, I.D., Kartali, S.I., Harding, R.M., Peto, T.E.A., and Crook, D.W. (2007) Diversity of antibiotic resistance integrative and conjugative elements among haemophili. *J Med Microbiol* **56:** 838–846.

Ditta, G., Stanfield, S., Corbin, D., and Helinski, D.R. (1980) Broad host range DNA cloning system for gram-negative bacteria: construction of a gene bank of *Rhizobium meliloti*. *Proc Natl Acad Sci USA* **77:** 7347–7351.

Drenkard, E., and Ausubel, F.M. (2002) *Pseudomonas* biofilm formation and antibiotic resistance are linked to phenotypic variation. *Nature* **416:** 740–743.

Everett, K.R., Taylor, R.K., Romberg, M.K., Rees-George, J., Fullerton, R.A., Vanneste, J.L., and Manning, M.A. (2011) First report of *Pseudomonas syringae* pv. *actinidiae* causing kiwifruit bacterial canker in New Zealand. *Australas Plant Dis Note* **6:** 67–71.

Fang, Y., Wu, L., Chen, G., and Feng, G. (2016) Complete genome sequence of *Pseudomonas azotoformans* S4, a potential biocontrol bacterium. *J Biotechnol* **227:** 25–26.

Feil, H., Feil, W.S., Chain, P., Larimer, F., Di Bartolo, G., Copeland, A., *et al*. (2005) Comparison of the complete genome sequences of *Pseudomonas syringae* pv. *syringae* B728a and pv. *tomato* DC3000. *Proc Natl Acad Sci USA* **102:** 11064–11069.

Fondi, M., Karkman, A., Tamminen, M.V., Bosi, E., Virta, M., Fani, R., *et al*. (2016) "Every gene is everywhere but the environment selects": global geolocalization of gene sharing in environmental samples through network analysis. *Genome Biol Evol* **8:** 1388–1400.

Garriss, G., Waldor, M.K., and Burrus, V. (2009) Mobile antibiotic resistance encoding elements promote their own diversity. *PLoS Genetic* **5:** e1000775.

Griffith, F. (1928) The significance of pneumococcal types. *J Hygiene* **27:** 113–159.

Guglielmini, J., Quintais, L., Garcillán-Barcia, M.P., de la Cruz, F., and Rocha, E.P. (2011) The repertoire of ICE in prokaryotes underscores the unity, diversity, and ubiquity of conjugation. *PLoS Genet* **7:** e1002222.

Gullberg, E., Albrecht, L.M., Karlsson, C., Sandegren, L., and Andersson, D.I. (2014) Selection of a multidrug resistance plasmid by sublethal levels of antibiotics and heavy metals. *mBio* **5:** 14–e01918.

Gutiérrez-Barranquero, J.A., de Vicente, A., Carrión, V.J., Sundin, G.W., and Cazorla, F.M. (2013) Recruitment and rearrangement of three different genetic determinants into a conjugative plasmid increase copper resistance in *Pseudomonas syringae*. *Appl Environ Microbiol* **79:** 1028–1033.

Hirano, S.S., and Upper, C.D. (2000) Bacteria in the leaf ecosystem with emphasis on *Pseudomonas syringae*—a pathogen, ice nucleus, and epiphyte. *Microbiol Mol Biol Rev* **64:** 624–653.

Holloway, B.W. (1955) Genetic recombination in *Pseudomonas aeruginosa*. *J Gen Microbiol* **13:** 572–581.

Hong, S., Candelone, J.P., Soutif, M., and Boutron, C.F. (1996) A reconstruction of changes in copper production and copper emissions to the atmosphere during the past 7000 years. *Sci Total Environ* **188:** 183–193.

Johnson, C.M., and Grossman, A.D. (2015) Integrative and conjugative elements (ICEs): what they do and how they work. *Annu Rev Genet* **49:** 577–601.

Juhas, M., Power, P.M., Harding, R.M., Ferguson, D.J., Dimopoulou, I.D., Elamin, A.R., *et al*. (2007) Sequence and functional analyses of *Haemophilus* spp. genomic islands. *Genome Biol* **8:** R237.

Kearse, M., Moir, R., Wilson, A., Stones-Havas, S., Cheung, M., Sturrock, S., *et al*. (2012) Geneious Basic: an integrated and extendable desktop software platform for the organization and analysis of sequence data. *Bioinformatics* **28:** 1647–1649.

Kung, V.L., Ozer, E.A., and Hauser, A.R. (2010) The accessory genome of *Pseudomonas aeruginosa*. *Microbiol Mol Biol Rev* **74:** 621–641.

Lan, R., and Reeves, P.R. (1996) Gene transfer is a major factor in bacterial evolution. *Mol Biol Evol* **13:** 47–55.

Lenski, R.E., Rose, M.R., Simpson, S.C., and Tadler, S.C. (1991) Long-term experimental evolution *in Escherichia coli*. I. Adaptation and divergence during 2,000 generations. *Am Nat* **138:** 1315–1341. –

Lilley, A.K., and Bailey, M.J. (1997) Impact of plasmid pQBR103 acquisition and carriage on the phytosphere fitness of *Pseudomonas fluorescens* SBW25: burden and benefit. *Appl Environ Microbiol* **63:** 1584–1587.

Lovell, H.C., Mansfield, J.W., Godfrey, S.A.C., Jackson, R.W., Hancock, J.T., and Arnold, D.L. (2009) Bacterial evolution by genomic island transfer occurs via DNA transformation *in planta*. *Curr Biol* **19:** 1586–1590.

McCann, H.C., Rikkerink, E.H.A., Bertels, F., Fiers, M., Lu, A., Rees-George, J., *et al*. (2013) Genomic analysis of the kiwifruit pathogen *Pseudomonas syringae* pv. *actinidiae* provides insight into the origins of an emergent plant disease. *PLoS Pathog* **9:** e1003503.

McCann, H.C., Li, L., Liu, Y., Li, D., Hui, P., Zhong, C., *et al*. (2017) Origin and evolution of the kiwifruit canker pandemic. *Gen Biol Evol* in press.

Mazzaglia, A., Studholme, D.J., Taratufolo, M.C., Cai, R., Almeida, N.F., Goodman, T., *et al*. (2012) *Pseudomonas syringae* pv. *actinidiae* (PSA) isolates from recent bacterial canker of kiwifruit outbreaks belong to the same genetic lineage. *PLoS One* **7:** e36518.

Médigue, C., Rouxel, T., Vigier, P., Hénaut, A., and Danchin, A. (1991) Evidence for horizontal gene transfer in *Escherichia coli* speciation. *J Mol Biol* **222:** 851–856.

Menkissoglu, O., and Lindow, S.E. (1991) Chemical forms of copper on leaves in relation to the bactericidal activity of cupric hydroxide deposits on plants. *Phytopathology* **81:** 1263–1270.

Mergeay, M., Monchy, S., Vallaeys, T., Auquier, V., Benotmane, A., Bertin, P., *et al*. (2003) *Ralstonia metallidurans*, a bacterium

specifically adapted to toxic metals: towards a catalogue of metal-responsive genes. *FEMS Microbiol Rev* **27:** 385–410.

Mohd-Zain, Z., Turner, S.L., Cerdeno-Tarraga, A.M., Lilley, A.K., Inzana, T.J., Duncan, A.J., *et al*. (2004) Transferable antibiotic resistance elements in *Haemophilus influenzae* share a common evolutionary origin with a diverse family of syntenic genomic islands. *J Bacteriol* **186:** 8114–8122.

Morgan, R.K., and Taylor, E. (2004) Copper accumulation in vineyard soils in New Zealand. *Environ Sci* **1:** 139–167.

Nakajima, M., Goto, M., and Hibi, T. (2002) Similarity between copper resistance genes from *Pseudomonas syringae* pv. *actinidiae* and *P. syringae* pv. *tomato*. *J Gen Plant Pathol* **68:** 68–74.

Neale, H.C., Laister, R., Payne, J., Preston, G., Jackson, R.W., and Arnold, D.L. (2016) A low frequency persistent reservoir of a genomic island in a pathogen population ensures island survival and improves pathogen fitness in a susceptible host. *Environ Microbiol*, **8:** 4144–4152.

Ochman, H., Lerat, E., and Daubin, V. (2005) Examining bacterial species under the specter of gene transfer and exchange. *Proc Natl Acad Sci USA* **102 (Suppl. 1):** 6595–6599.

Ochman, H., Lawrence, J.G., and Groisman, E.A. (2000) Lateral gene transfer and the nature of bacterial innovation. *Nature* **405:** 299–304.

Peters, S.E., Hobman, J.L., Strike, P., and Ritchie, D.A. (1991) Novel mercury resistance determinants carried by IncJ plasmids pMERPH and R391. *Mol Gen Genet* **228:** 294–299.

Pitman, A.R., Jackson, R.W., Mansfield, J.W., Kaitell, V., Thwaites, R., and Arnold, D.L. (2005) Exposure to host resistance mechanisms drives evolution of bacterial virulence in plants. *Curr Biol* **15:** 2230–2235.

Polz, M.F., Alm, E.J., and Hanage, W.P. (2013) Horizontal gene transfer and the evolution of bacterial and archaeal population structure. *Trends Genet* **29:** 170–175.

Popa, O., and Dagan, T. (2011) Trends and barriers to lateral gene transfer in prokaryotes. *Curr Opin Microbiol* **14:** 615–623.

Quiroz, T.S., Nieto, P.A., Tobar, H.E., Salazar-Echegarai, F.J., Lizana, R.J., Quezada, C.P., *et al*. (2011) Excision of an unstable pathogenicity island in *Salmonella enterica* serovar *enteritidis* is induced during infection of phagocytic cells. *PLoS One* **6:** e26031.

Ramsay, J.P., Sullivan, J.T., Stuart, G.S., Lamont, I.L., and Ronson, C.W. (2006) Excision and transfer of the *Mesorhizobium loti* R7A symbiosis island requires an integrase IntS, a novel recombination directionality factor RdfS, and a putative relaxase RlxS. *Mol Microbiol* **62:** 723–734.

Rauch, P.J.G., and De Vos, W.M. (1992) Characterization of the novel nisin-sucrose conjugative transposonTn5276 and its insertion in *Lactococcus lactis*. *J Bacteriol* **174:** 1280–1287.

Ravatn, R., Studer, S., Springael, D., Zehnder, A.J.B., and Van Der Meer, J.R. (1998) Chromosomal integration, tandem amplification, and deamplification in *Pseudomonas putida* F1 of a 105-kilobase genetic element containing the chlorocathecol degradative genes from *Pseudomonas* sp. strain B13. *J Bacteriol* **180:** 4360–4369.

Rees-George, J., Vanneste, J.L., Cornish, D.A., Pushparajah, I.P.S., Yu, J., Templeton, M.D., and Everett, K.R. (2010) Detection of *Pseudomonas syringae* pv. *actinidiae* using polymerase chain reaction (PCR) primers based on the 16S-23S rDNA intertranscribed spacer region and comparison with PCR primers based on other gene regions. *Plant Pathol* **59:** 453–464.

Rensing, C., and Grass, G. (2003) *Escherichia coli* mechanisms of copper homeostasis in a changing environment. *FEMS Microbiol Rev* **27:** 197–213.

Roberts, A.P., and Mullany, P. (2009) A modular master on the move: the Tn916 family of mobile genetic elements. *Trends Microbiol* **17:** 251–258.

Retchless, A.C., and Lawrence, J.G. (2007) Temporal fragmentation of speciation in bacteria. *Science* **317:** 1093–1096.

Ruinelli, M., Schneeberger, P.H.H., Ferrante, P., Bühlmann, A., Scortichini, M., Vanneste, J.L., *et al*. (2017) Comparative genomics-informed design of two LAMP assays for detection of the kiwifruit pathogen Pseudomonas syringae pv. actinidiae and discrimination of isolates belonging to the pandemic biovar 3. *Plant Pathol* **66:** 140–149.

Staehlin, B.M., Gibbons, J.G., Rokas, A., O'halloran, T.V., and Slot, J.C. (2016) Evolution of a heavy metal homeostasis/resistance island reflects increasing copper stress in *Enterobacteria*. *Genome Biol Evol* **8:** 811–826.

Stoesser, N., Giess, A., Batty, E.M., Sheppard, A.E., Walker, A.S., Wilson, D.J., *et al*. (2014) Genome sequencing of an extended series of NDM-producing *Klebsiella pneumoniae* isolates from neonatal infections in a Nepali hospital characterizes the extent of community- versus hospital-associated transmission in an endemic setting. *Antimicrob Agents Chemother* **58:** 7347–7357.

Sullivan, J.T., and Ronson, C.W. (1998) Evolution of rhizobia by acquisition of a 500-kb symbiosis island that integrates into a phe-tRNA gene. *Proc Natl Acad Sci USA* **95:** 5145–5514.

Sullivan, J.T., Patrick, H.N., Lowther, W.L., Scott, D.B., and Ronson, C.W. (1995) Nodulating strains of *Rhizobium loti* arise through chromosomal symbiotic gene transfer in the environment. *Proc Natl Acad Sci USA* **92:** 8985–8989.

Sundin, G.W., Jones, A.L., and Fulbright, D.W. (1989) Copper resistance in *Pseudomonas syringae* pv. *syringae* from cherry orchards and its associated transfer *in vitro* and *in planta* with a plasmid. *Phytopathology* **79:** 861–865.

Templeton, M.D., Warren, B.A., Andersen, M.T., Rikkerink, E.H.A., and Fineran, P.C. (2015) Complete DNA sequence of *Pseudomonas syringae* pv. *actinidiae*, the causal agent of kiwifruit canker disease. *Genome Announc* **3:** e01054-15.

Teverson, D.M. (1991) Genetics of pathogenicity and resistance in the halo-blight disease of beans in Africa. Ph.D. thesis. Birmingham, United Kingdom: University of Birmingham.

Vanga, B.R., Ramakrishnan, P., Butler, R.C., Toth, I.K., Ronson, C.W., Jacobs, J.M.E., and Pitman, A.R. (2015) Mobilization of horizontally acquired island 2 is induced in plantain the phytopathogen *Pectobacterium atrosepticum* SCRI1043 and involves the putative relaxase

ECA0613 and quorum sensing. *Environ Microbiol* **17:** 4730–4744.

Vanneste, J.L., Giovanardi, D., Yu, J., Cornish, D.A., Kay, C., Spinelli, F., and Stefani, E. (2011) Detection of *Pseudomonas syringae* pv. *actinidiae* in kiwifruit pollen samples. *N Z Plant Protect* **64:** 246–251.

Visnovsky, S.B., Fiers, M., Lu, A., Panda, P., Taylor, R., and Pitman, A.R. (2016) Draft genome sequences of 18 strains of *Pseudomonas* isolated from kiwifruit plants in New Zealand and overseas. *Genome Announc* **4:** e00061–e00016.

Wozniak, R.A.F., and Waldor, M.K. (2010) Integrative and conjugative elements: mosaic mobile genetic elements enabling dynamic lateral gene flow. *Nat Rev Microbiol* **8:** 552–563.

Zhang, X.X., George, A., Bailey, M.J., and Rainey, P.B. (2006) The histidine utilization (*hut*) genes of *Pseudomonas fluorescens* SBW25 are active on plant surfaces, but are not required for competitive colonization of sugar beet seedlings. *Microbiology* **152:** 1867–1875.

Zhang, X.X., Gauntlett, J.C., Oldenburg, D.G., Cook, G.M., and Rainey, P.B. (2015) role of the transporter-like sensor kinase CbrA in histidine uptake and signal transduction. *J Bacteriol* **197:** 2867–2878.

Supporting information

Additional Supporting Information may be found in the online version of this article at the publisher's web-site

Fig. S1. New Zealand kiwifruit growing regions with isolation sites of copper resistant *Psa*. Map was modified from regional classification map of June 2016 (Kiwi Vine Health (KVH)).

Fig. S2. UPMGA tree of the Cus system proteins in *Psa* NZ. Bootstrap values are shown at each node.

Fig. S3. UPMGA trees of the Cop proteins genes in *Psa* NZ. Bootstrap values are shown at each node.

Fig. S4. UPMGA trees of CopR and CopS proteins in *Psa* NZ. Bootstrap values are shown at each node.

Fig. S5. Density of single and co-cultured *Psa* in liquid MGY supplemented with 0.5 m and 0.8 mM $CuSO_4$. *Psa* NZ13 was cultured alone (white bars) or co-cultured with *Psa* NZ45 (grey bars). Data are means and standard deviation of three independent cultures. Asterisk indicates significance at 5% level by one-tailed *t*-test.

Fig. S6. *In planta* growth of *Psa* NZ13 and *Psa* NZ45. The single growth of *Psa* NZ13 (white bars) and *Psa* NZ45 (grey bars) was assessed endophytically on leaves of the kiwifruit cultivar Hort16A. The copper product Nordox75 (0.375 g l^{-1}) was sprayed adaxially and abaxially until run off. Data are means and standard deviation of five replicates. One tailed *t*-test showed no statistical difference in growth between of *Psa* NZ13 and NZ45 in absence or presence of copper.

Fig. S7. Growth of co-inoculated *Psa* NZ13 and *Psa* NZ45 on kiwifruit leaves. Growth of *Psa* NZ13 (white bars) and *Psa* NZ45 (grey bars) was assessed endophytically (A) and epiphytically (B) on leaves of the kiwifruit cultivar Hort16A. The copper product Nordox75 (0.375 g L^{-1}) was sprayed adaxially and abaxially until run off. Data are means and standard deviation of five replicates. One tailed *t*-test showed no statistical difference in growth between of *Psa* NZ13 and NZ45 in absence or presence of copper.

Fig. S8. Analysis of the presence of the variable region (VR) of Psa_{NZ45}ICE_Cu and Psa_{NZ13}ICE_eno in 11 *Psa* NZ13 transconjugants. PCRs were carried out to detect *copA* (VR of Psa_{NZ45}ICE_Cu) or *enolase* genes (VR of Psa_{NZ13}ICE_eno). Controls of *Psa* NZ13 and *Psa* NZ45 show one and two bands, indiciative of Psa_{NZ13}ICE_eno in *Psa* NZ13 and both Psa_{NZ13}ICE_eno Psa_{NZ45}ICE_Cu and in *Psa* NZ45, respectively. All transconjugants, lanes 1–11 have acquired Psa_{NZ45}ICE_Cu.

Fig. S9. Analysis of the insertion site of the Psa_{NZ13}ICE_eno and Psa_{NZ45}ICE_Cu in 11 *Psa* NZ13 transconjugants. PCRs were to detect the integration of Psa_{NZ13}ICE_eno in the *att-1* or *att-2* sites (*intPsaNZ13-att-1* and *intPsaNZ13-att-2*) and the integration of Psa_{NZ45}ICE_Cu in the *att-1* or *att-2* sites (*intPsaNZ45-att-1* and *intPsaNZ45-att-2*). Controls of *Psa* NZ13 and *Psa* NZ45 show that in *Psa* NZ13 the Psa_{NZ13}ICE_eno is integrated in the *att-1* site and in *Psa* NZ45 the Psa_{NZ13}ICE_eno is integrated in the *att-1* and the Psa_{NZ45}ICE_Cu in the *att-2* site.

Table S1. *In planta* transfer of Psa_{NZ45}ICE_cu from *Psa* NZ45 to *Psa* NZ13 at different founding ratios of donor and recipient. Donor and recipient strains were dip-inoculated onto Hort16A leaves at different founding ratios and frequency of recipients determined at days 3 and 7.

Table S2. Primers used for Psa_{NZ13}ICE_eno and Psa_{NZ45}ICE_Cu detection and integration loci.